Phonon Screening in High-Temperature Superconductors

C. C. Homes,[1,*] A. W. McConnell,[2] B. P. Clayman,[2] D. A. Bonn,[3] Ruixing Liang,[3] W. N. Hardy,[3] M. Inoue,[4] H. Negishi,[4] P. Fournier,[5] and R. L. Greene[5]

[1]*Department of Physics, Brookhaven National Laboratory, Upton, New York 11973*
[2]*Department of Physics, Simon Fraser University, Burnaby, British Columbia, Canada V5A 1S6*
[3]*Department of Physics and Astronomy, University of British Columbia, Vancouver, British Columbia, Canada V6T 1Z1*
[4]*Graduate School of Advanced Sciences of Matter, Hiroshima University, Higashi-Hiroshima 739-8526, Japan*
[5]*Center for Superconductivity Research, Department of Physics and Astronomy, University of Maryland, College Park, Maryland 20742*

(Received 11 June 1999; revised manuscript received 28 December 1999)

In good conductors optical phonons are usually screened, and therefore not observed. However, sharp features due to infrared-active modes in the copper-oxygen planes are observed in the optical conductivity of $Pr_{1.85}Ce_{0.15}CuO_4$ and $YBa_2Cu_3O_{6.95}$. Oscillator strengths indicate that the screening of these modes is poor or totally absent. These materials are compared with η-Mo_4O_{11}, in which lattice modes appear suddenly below the charge-density wave transition. It is proposed that poor screening in the cuprates originates from fluctuating charge inhomogeneities in the copper-oxygen planes.

PACS numbers: 74.25.Kc, 74.25.Gz, 74.72.–h

Since the discovery of superconductivity at elevated temperatures in the cuprate family of materials, there has been considerable study and debate as to the role (if any) that the phonons play in these systems [1,2]. In the past, detailed optical studies of phonons in the superconducting cuprates have been primarily along the poorly conducting c-axis direction [3–5]. Optical studies of the in-plane lattice modes have been mainly Raman scattering experiments. The failure in the past to observe optical phonons in the highly conducting copper-oxygen planes has been attributed to the presence of screening currents due to the free carriers [1]. It is generally accepted that the lattice modes are only weakly coupled to the free carriers [6].

In this Letter we present evidence that the infrared-active lattice modes in the cuprates are generally poorly screened, or totally *unscreened* in the conducting copper-oxygen planes.

These systems are compared with the model system η-Mo_4O_{11} in which the lattice modes are effectively screened [7] until an incommensurate charge-density wave (CDW) forms. This suggests that the anomalous behavior may be related to fluctuating charge inhomogeneities in the copper-oxygen planes, similar to the static charge-ordered phase which has been observed in some of the nickelates [8].

For phonons to be optically active requires an induced dipole moment that can couple to electromagnetic radiation. In strongly ionic materials, like the alkali-halide salts, the formal charge is localized on the ions, which together with the absence of any free carriers results in the strong optical activity of the optic ("Reststrahlen") mode. The strength ($\propto \omega_p^2$) of the transverse optic mode (ω_{TO}) is related to the position of the longitudinal optic mode (ω_{LO}) by $\omega_p^2 = \epsilon_\infty(\omega_{\mathrm{LO}}^2 - \omega_{\mathrm{TO}}^2)$, where the splitting of the transverse and longitudinal modes are related to the static and core values of the dielectric function by the Lyddane-Sachs-Teller relation $\omega_{\mathrm{LO}}^2/\omega_{\mathrm{TO}}^2 = \epsilon_0/\epsilon_\infty$. In a metallic system, screening effects dramatically reduce ω_{LO}, resulting in reduced splitting and a decrease in the strength of the optic mode. In general, in a covalent system, if the electronic (Drude) plasma frequency of the carriers ($\omega_{pD}^2 = 4\pi n e^2/m^*$, where n is the carrier density and m^* is the effective mass) is much greater than the frequencies of the lattice vibrations, then the Thomas-Fermi dielectric constant $\epsilon_{TF}(\omega, \mathbf{q} = 0) \simeq 1 - \omega_{pD}^2/\omega^2$ is appropriate [9]. The screened Coulomb potential $U(r) = (Z/r)e^{-r/l_s}$ corresponds to a screening length

$$l_s^2 = \frac{a_0}{4}\left(\frac{\pi}{3n}\right)^{1/3}, \tag{1}$$

where a_0 is the Bohr radius. This form of the potential decreases quickly to a negligible size at a distance greater than l_s. For copper, $n \approx 8.5 \times 10^{22}$ cm^{-3} yields $l_s \approx 0.6$ Å, which is much less than the nearest-neighbor distance ($\approx$2.5 Å), indicating that the cores are heavily screened from each other. In a covalent system where the charge is delocalized and the ionic cores are screened, the optical phonons are expected to be very weak (i.e., a feature of less than 0.01% when the reflectance is close to unity).

Initial reflectance studies of the high-temperature cuprate superconductors emphasized signal-to-noise over resolution in an attempt to accurately determine the reflectance at low frequency [6]. However, recent refinements in which the entire face of the crystal may be studied [10] allow sufficient signal-to-noise in the reflectance (better than 1000:1) at high resolution ($\leq$2 cm^{-1}) to resolve weak spectral features in small samples of $Pr_{1.85}Ce_{0.15}CuO_4$, and detwinned $YBa_2Cu_3O_{6.95}$, where the reflectance is near unity.

The temperature dependent reflectance of the hole-doped $YBa_2Cu_3O_{6.95}$ material has been measured

over a wide frequency range for light polarized along the a direction (which probes just the CuO_2 planes) [11], and for the electron-doped $Pr_{1.85}Ce_{0.15}CuO_4$ material for light polarized in the a-b plane [12]. The spectral resolution in each case is 2 cm^{-1}. Both materials are optimally doped with respect to T_c. The optical conductivity has been calculated from a Kramers-Kronig analysis, and the results are shown in the upper and lower panels of Fig. 1 for the hole- and electron-doped materials, respectively. In $YBa_2Cu_3O_{6.95}$ the overall behavior of the conductivity is similar to other studies [13] and has been discussed in a separate publication [11]. However, there are also three clearly discernible peaks in the room-temperature conductivity, which narrow with decreasing temperature. The optical conductivity of $Pr_{1.85}Ce_{0.15}CuO_4$ is more complicated. While there is only one strong feature at room temperature, there are several weak, broad features that become sharper at low temperature. In both systems, these are modes that are very close, or identical to, the infrared-active vibrations observed in the undoped materials [14,15], and are therefore assigned as the infrared-active

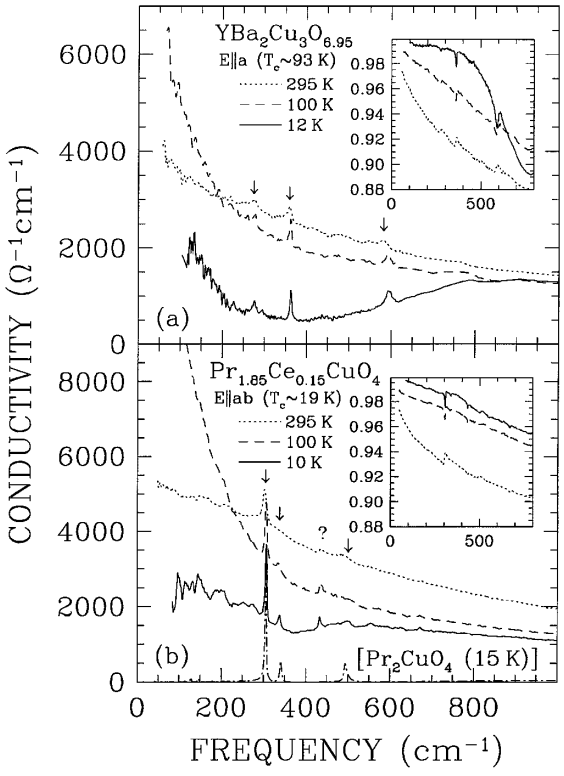

FIG. 1. (a) The real part of the optical conductivity of $YBa_2Cu_3O_{6.95}$ for light polarized along the a axis at 295, 100, and 12 K from ≈50 to 1000 cm^{-1}. The arrows indicate the positions of the infrared-active B_{3u} vibrations associated with the E_u modes observed in undoped $YBa_2Cu_3O_6$. Inset: The reflectance. (b) The optical conductivity of $Pr_{1.85}Ce_{0.15}CuO_4$ for light polarized in the a-b plane at 295, 100, and 10 K. The arrows indicate the positions of the infrared-active vibrations associated with the E_u modes in insulating Pr_2CuO_4, which is shown at the bottom of the plot (dash-dotted line) at ≈15 K. Inset: The reflectance of $Pr_{1.85}Ce_{0.15}CuO_4$. The spectral resolution in all panels is 2 cm^{-1}.

B_{3u} and E_u modes in the hole- and electron-doped materials, respectively [16]. The low-frequency modes observed in the insulators are too weak to be observed in the doped systems with the current signal-to-noise ratio.

The phonons have been fit using a series of Lorentzian oscillators

$$\sigma_1(\omega) = \frac{1}{60}\sum_j \frac{\omega_{p,j}^2 \omega^2 \gamma_j}{(\omega_j^2 - \omega^2)^2 + \omega^2\gamma_j^2} \qquad (\Omega^{-1}\ \mathrm{cm}^{-1}), \tag{2}$$

where w_j, γ_j, and $\omega_{p,j}$ are the frequency, width, and effective plasma frequency of the jth vibration. The dimensionless oscillator strength is written as $S_j = \omega_{p,j}^2/\omega_j^2$. The results of the fits using simple linear backgrounds are listed in Table I, and compared with the phonon parameters that have been observed for the undoped systems [15]. In the electron-doped system, the oscillator strengths of all of the observed infrared-active vibrations have decreased slightly in the presence of doped carriers ($S_j^d/S_j^u \approx 0.8$, where "d" and "u" refer to the doped and undoped systems, respectively). However, in the hole-doped $YBa_2Cu_3O_{6.95}$ material $S_j^d/S_j^u > 1$ for all of the infrared-active modes, indicating that there is *no* screening. One mode in particular at 275 cm^{-1} shows a dramatic enhancement of the oscillator strength, $S_j^d/S_j^u \approx 2.2$; this mode involves mainly the oxygen displacements in the copper-oxygen planes rather than the chain sites [17], into which the oxygen dopes. This unexpected behavior suggests that the lattice modes in the hole-doped material respond to the doped carriers in a very unusual way.

Using the behavior of the two-dimensional (2D) incommensurate CDW system η-Mo_4O_{11} as a model, it

TABLE I. The fitted phonon parameters of the observable vibrational features in $YBa_2Cu_3O_{6.95}$ and $Pr_{1.85}Ce_{0.15}CuO_4$ for the electric field parallel to the a and a-b planes, respectively (CuO_2 planes *only*) at 295 K (see Fig. 1). (All units are in cm^{-1}, except for the dimensionless oscillator strength $S_j = \omega_{p,j}^2/\omega_j^2$; u and d refer to the undoped and doped materials, respectively.)

$YBa_2Cu_3O_6$ (E_u)[a]				$YBa_2Cu_3O_{6.95}$ (B_{3u})				
ω_j	γ_j	$\omega_{p,j}$	(S_j^u)	ω_j	γ_j	$\omega_{p,j}$	(S_j^d)	S_j^d/S_j^u
118	9	121	(1.05)	⋯	⋯	⋯	(⋯)	(⋯)
193	10	164	(0.75)	⋯	⋯	⋯	(⋯)	(⋯)
250	14	231	(0.85)	275	20	378	(1.89)	2.22
357	30	449	(1.55)	360	12	460	(1.64)	1.06
588	26	415	(0.50)	581	23	479	(0.68)	1.33
Pr_2CuO_4 (E_u)[b]				$Pr_{1.85}Ce_{0.15}CuO_4$ (E_u)[c]				
ω_j	γ_j	$\omega_{p,j}$	(S_j^u)	ω_j	γ_j	$\omega_{p,j}$	(S_j^d)	S_j^d/S_j^u
131	4	161	(1.52)	⋯	⋯	⋯	(⋯)	(⋯)
302	10	790	(6.84)	306	4	739	(5.83)	0.85
331	14	353	(1.13)	338	6	348	(1.06)	0.93
489	25	475	(0.95)	500	16	364	(0.53)	0.55

[a]Reference [15].
[b]This work.
[c]The results of the fits at 10 K are shown, as the modes at 338 and 500 cm^{-1} are quite broad at room temperature.

is proposed that these features may be explained by the presence of fluctuating charge inhomogeneities [7]. The free carriers in η-Mo_4O_{11} are known to be confined in the b-c planes, resulting in quasi-2D electronic properties [18]. This material undergoes incommensurate CDW transitions at $T_{c1} \approx 110$ K with an incommensurate CDW modulation of $\boldsymbol{q} = 0.23b^*$, and $T_{c2} \approx 35$ K [$\boldsymbol{q} = (0.42b^*, 0.28c^*)$]. These CDW transitions are observed primarily in transport [19], having only weak structural distortions associated with the transitions [20]. However, the Fermi surface is only partially gapped so that the general trend is that the material continues to become *more* metallic with decreasing temperature. As Fig. 2(a) shows, at 115 K ($T \gtrsim T_{c1}$) the conductivity is quite high, and there is no sign of optical phonons in either the optical conductivity, or the reflectance (shown in the inset). Despite the absence of features in the reflectance, weak absorptions in the powder absorption spectra have been identified as infrared-active lattice modes [21].

At 115 K, the observed carrier concentration in η-Mo_4O_{11} is $n \approx 2 \times 10^{22}$ cm^{-3} [19], or $l_s \approx 0.7$ Å, comparable to the screening length in copper (≈0.6 Å). At 85 K ($T_{c2} < T < T_{c1}$), a dramatic change occurs; while the overall value of the low-frequency reflectance has changed by less than 0.5%, a variety of new, sharp spectral features have appeared in the reflectance and the conductivity, as shown in Fig. 2(b). Some of these features are the normally active infrared modes which have been observed above T_{c1} in powder transmission experiments [21]. However, there is new structure as well. The presence of strong features in the conductivity below T_{c1} is surprising given the absence of a fully gapped Fermi surface, only a slight decrease in the conductivity, and a high carrier concentration [19] of $n \approx 6 \times 10^{21}$ cm^{-3} ($l_s \approx 0.9$ Å). This suggests that the screened lattice modes become suddenly visible either as a result of the incommensurate CDW altering the nature of the screening currents, or in the case of new structure [21] by allowing lattice modes to couple to the charge modulation created by the incommensurate CDW. This latter behavior has been extensively studied in the one-dimensional (1D) molecular crystals with CDW distortions, where the totally symmetric vibrations are activated as "phase phonons" (phase oscillations of the stabilizing CDW) which arise from the linear coupling of the modes to the conduction electron molecular orbital [22].

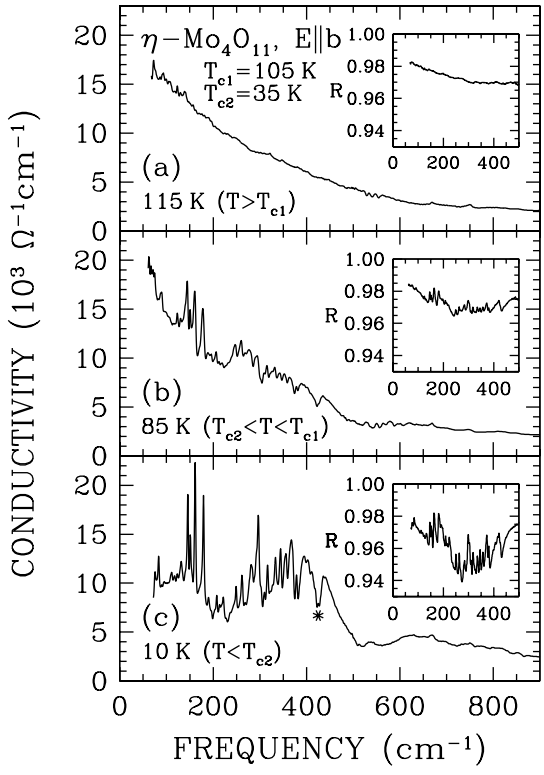

FIG. 2. (a) The real part of the optical conductivity of η-Mo_4O_{11} for light polarized along the b axis from ≈50 to 1000 cm^{-1} at 115 K. Inset: The reflectance. (b) The real part of the conductivity below T_{c1} at 85 K, showing a number of sharp resonances superimposed upon a high background conductivity. Inset: The reflectance. (c) The real part of the conductivity below T_{c2} at 10 K, where a large number of spectral features can now be resolved. The clearest example of an antiresonance is at ≈420 cm^{-1} (asterisk). Inset: The reflectance. The spectral resolution for all three data sets is 2 cm^{-1}.

An attribute of phase phonons is that they appear as resonances in the conductivity below the gap energies, and as antiresonances above [22]. The low-frequency modes in Fig. 2(b) ($\lesssim$200 cm^{-1}) have the appearance of resonances, while at high frequency ($\omega \gtrsim 350$ cm^{-1}), the modes appear to be antiresonances, in agreement with estimates for the maximum value of the gap in this material of $2\Delta_{max} \approx 270$ cm^{-1} [7]. The clearest example of an antiresonance is at low temperature in Fig. 2(c) at ≈420 cm^{-1}, but it is possible that there are others as well. Phase phonons often display enhanced oscillator strengths, and several of the modes in Fig. 2(c) have oscillator strengths that are much larger than those typically seen in other transition-metal oxides [7,15], suggesting that they may couple to the CDW.

In $Pr_{1.85}Ce_{0.15}CuO_4$, the carrier concentration has been estimated at $n \approx 1 \times 10^{22}$ cm^{-3} [23], which yields $l_s \approx 0.8$ Å. While some screening occurs in the electron-doped material, the phonons are still clearly visible. In YBa_2Cu_3-$O_{7-\delta}$ just above T_c, the carrier concentration has been determined to be $n \approx 6 \times 10^{21}$ cm^{-3} [24]; if half of the carriers reside in the CuO_2 planes, this yields a screening length of $l_s \approx 1$ Å, comparable to the screening length in η-Mo_4O_{11} above and below T_{c1}. The values of l_s in the cuprates are close to those observed in η-Mo_4O_{11}. However, the lattice modes in η-Mo_4O_{11} become unscreened not due to a dramatic increase in l_s, but due to the formation of a CDW. It therefore seems likely that the poor or total absence of screening in the cuprates is also due to the presence of some charge inhomogeneity in the CuO_2 planes. There is considerable evidence for charge inhomogeneities in the cuprates [25]. However, it

has also been suggested that any charge inhomogeneities in the cuprates are a dynamical effect, rather than a static one [8].

An inhomogeneous charge distribution in the CuO_2 planes may allow the observation of normally screened modes by (i) altering the path of the screening currents in such a way that the ionic cores are no longer effectively screened, (ii) altering the nature of the transport to a "diffusive" process in which the carriers move much more slowly than the ionic cores, thereby allowing the lattice modes to couple to the infrared radiation, or (iii) by allowing the lattice modes to couple directly to the charge structures, in a manner similar to the phase phonons observed in η-Mo_4O_{11}.

In the first instance, charge inhomogeneities in the CuO_2 planes (a "stripe" phase) may lead to "carrier-rich" and "carrier-poor" regions [8]; if screening currents move effectively only in the carrier-rich regions, then the ionic cores will no longer be effectively screened, leading to absorption. On the other hand, there is good evidence that the transport in the CuO_2 planes is not that of a Fermi liquid [26], so that charge inhomogeneities may result in transport properties where the carrier movement is very slow (diffusive) with respect to the motion of the ionic cores. Thus, the carriers will not be able to effectively screen the induced-dipole moment, and the phonons will be optically active. Finally, it may be possible that some lattice modes are coupling directly with a dynamical charge modulation, regardless of whether screening currents are present or not. This mechanism may explain the increase in oscillator strength with doping of the 275 cm^{-1} mode in $YBa_2Cu_3O_{6.95}$. However, the majority of the lattice modes have oscillator strengths similar to those found in the insulating materials [15], so that if there is coupling to charge structures, it is in all likelihood of a different nature than is found in the 1D systems. Note that *all* of these arguments assume that the dynamical charge inhomogeneities or charge modulation occurs much more slowly than the motion of the ionic cores.

In summary, we have presented evidence for very poor screening of the infrared-active lattice modes in the highly conducting CuO_2 planes of $Pr_{1.85}Ce_{0.15}CuO_4$, and a total absence of screening of these modes in $YBa_2Cu_3O_{6.95}$. It is likely that this optical activity has its origins in dynamical charge inhomogeneities, which change on a time scale much longer than the lattice vibrations. The mode at 275 cm^{-1} in $YBa_2Cu_3O_{6.95}$ may also couple to these inhomogeneities, resulting in an increase of oscillator strength. The slight difference in the degree of screening between electron- and hole-doped materials may indicate that electrons and holes behave differently in the cuprates. Infrared-active lattice modes may provide a unique tool with which to probe the charge dynamics in this interesting class of materials.

We thank D. N. Basov, V. J. Emery, P. F. Henning, M. Strongin, and J. M. Tranquada for many helpful discussions. This work was supported by the Natural Sciences and Engineering Research Council of Canada, the Canadian Institute for Advanced Research, and the Department of Energy under Contract No. DE-AC02-98CH10886. The work in Maryland is supported by the NSF Condensed Matter Physics Division under Grant No. DMR 9732736.

*Electronic address: homes@bnl.gov

[1] A. P. Litvinchuck, C. Thomson, and M. Cardona, in *Physical Properties of High-Temperature Superconductors IV,* edited by D. M. Ginsberg (World Scientific, Singapore, 1994).
[2] T. Egami and S. J. L. Billinge, in *Physical Properties of High-Temperature Superconductors V,* edited by D. M. Ginsberg (World Scientific, Singapore, 1996).
[3] C. C. Homes *et al.,* Physica (Amsterdam) **254C**, 265 (1995).
[4] J. Schützmann *et al.,* Phys. Rev. B **52,** 13 665 (1995).
[5] S. Uchida, K. Tamasaku, and S. Tajima, Phys. Rev. B **53,** 14 558 (1996).
[6] D. B. Tanner and T. Timusk, in *Physical Properties of High-Temperature Superconductors III,* edited by D. M. Ginsberg (World Scientific, Singapore, 1992).
[7] A. W. McConnell *et al.,* Phys. Rev. B **58,** 13 565 (1998); A. W. McConnell, Ph.D. thesis, Simon Fraser University, 1999; a more recent measurement of the reflectance of η-Mo_4O_{11} for light polarized along the *b* axis is shown here.
[8] J. M. Tranquada *et al.,* Phys. Rev. Lett. **78,** 338 (1997).
[9] R. A. Cowley and G. Dolling, Phys. Rev. Lett. **14**, 549 (1965).
[10] C. C. Homes, M. Reedyk, D. Crandles, and T. Timusk, Appl. Opt. **32,** 2972 (1993).
[11] C. C. Homes *et al.,* Phys. Rev. B **60**, 9782 (1999).
[12] The reflectance of the electron-doped superconductor $Pr_{1.85}Ce_{0.15}CuO_4$ and the insulating parent material Pr_2CuO_4 have been measured over a wide frequency range at a variety of temperatures. The optical conductivity has been determined from a Kramers-Kronig analysis.
[13] D. N. Basov *et al.,* Phys. Rev. Lett. **74**, 598 (1995).
[14] M. K. Crawford *et al.,* Phys. Rev. B **41**, 8933 (1990).
[15] S. Tajima *et al.,* Phys. Rev. B **43,** 10 496 (1991).
[16] J. Humlíček *et al.,* Physica (Amsterdam) **206C**, 345 (1993).
[17] R. Liu *et al.,* Phys. Rev. B **37**, 7971 (1988).
[18] M. Ghedira *et al.,* J. Solid State Chem. **56,** 66 (1985).
[19] M. Sasaki, G. X. Tai, S. Tamura, and M. Inoue, Phys. Rev. B **47**, 6216 (1993).
[20] H. Guyot *et al.,* J. Phys. C **18,** 4427 (1985).
[21] Z. Zhu *et al.,* Synth. Met. **103,** 2238 (1999).
[22] M. J. Rice, Phys. Rev. Lett. **37**, 36 (1976).
[23] S. J. Hagen, J. L. Peng, Z. Y. Li, and R. L. Greene, Phys. Rev. B **43,** 13 606 (1991).
[24] T. R. Chien, D. A. Brawner, Z. Z. Wang, and N. P. Ong, Phys. Rev. B **43,** R6242 (1991).
[25] V. J. Emery and S. A. Kivelson, Physica (Amsterdam) **235–240C**, 189 (1994).
[26] A. T. Zheleznyak, V. M. Yakovenko, H. D. Drew, and I. I. Mazin, Phys. Rev. B **57,** 3089 (1998).